



Three-dimensional fat-saturated T1-weighted Cartesian volumetric interpolated breath-hold examination (VIBE) for the diagnosis of aortitis in patients with suspected large vessel vasculitis: a comparative study with ^{18}F -FDG PET applying fully integrated PET/MRI

I. Einspieler^{a,b,c,*}, M. Henninger^a, V. Mergen^a, H. Wendorff^d, B. Haller^e, M. Eiber^a, E.J. Rummeny^b, M. Schwaiger^a, P. Moog^{f,1}, K. Thürmel^{f,1}

^a Department of Nuclear Medicine, Technische Universität München, Klinikum rechts der Isar, Munich, Germany

^b Department of Radiology, Technische Universität München, Klinikum rechts der Isar, Munich, Germany

^c Department of Radiology, University Hospital Regensburg, Regensburg, Germany

^d Department of Vascular Surgery, Technische Universität München, Klinikum rechts der Isar, Munich, Germany

^e Department of Medical Statistics and Epidemiology, Technische Universität München, Klinikum rechts der Isar, Munich, Germany

^f Department of Nephrology and Rheumatology, Technische Universität München, Klinikum rechts der Isar, Munich, Germany

ARTICLE INFORMATION

Article history:

Received 4 February 2019

Accepted 11 April 2019

AIM: To evaluate the feasibility of T1-weighted (T1W) three-dimensional (3D) fat saturated Cartesian volumetric interpolated breath-hold examination (VIBE) magnetic resonance imaging (MRI) sequence for the diagnosis of aortitis in patients with suspected large vessel vasculitis (LVV) applying fully integrated 2- ^{18}F -fluoro-2-deoxy-D-glucose (^{18}F -FDG) positron-emission tomography (PET)/MRI.

MATERIAL AND METHODS: Fourteen patients with aortitis and 14 patients with a negative study for aortitis using ^{18}F -FDG PET as the standard of reference for the evaluation of inflammatory aortic involvement were included retrospectively. All patients were imaged at 3 T using T1W VIBE pre- and post-contrast. Four aortic segments were evaluated for image quality (IQ), diagnostic confidence (DC), and the degree of inflammatory activity (IA) using a Likert scale. Binomial and generalised estimating equation model tests were used to assess the diagnostic performance of T1W VIBE. Cohen's *k* was applied to test for interobserver reproducibility with respect to IA. Spearman's rank correlation coefficient was calculated to examine correlations between IQ, DC, IA, and PET results.

* Guarantor and correspondent: I. Einspieler, University Hospital Regensburg, Franz-Josef-Strauß-Allee 11, 93053 Regensburg, Germany. Tel.: +49 941 944 17493.

E-mail address: ingo.einspieler@ukr.de (I. Einspieler).

¹ These authors share last authorship.

RESULTS: On a patient- and segment-based analysis, sensitivity, specificity, positive predictive value, negative predictive value, and accuracy were 85.7% and 59.8%, 100% and 100%, 100% and 100%, 87.5% and 68%, and 92.9% and 82.1%, respectively. IQ and DC were acceptable to good in all examinations and substantial interobserver agreement was observed for IA (Cohen's $k = 0.69$). IQ and DC as well as IA and ^{18}F -FDG vessel wall uptake were significantly correlated ($r=0.763$ and 0.679 , respectively; $p<0.0001$).

CONCLUSION: T1W 3D fat saturated VIBE MRI allows diagnosis of aortitis and may aid in the management of patients with suspected LVV.

© 2019 The Royal College of Radiologists. Published by Elsevier Ltd. All rights reserved.

Introduction

Aortitis is a common manifestation of large vessel vasculitis (LVV) with giant-cell arteritis (GCA) and Takayasu arteritis (TA) as the two main variants. Early detection of extracranial LVV, including aortitis with a prevalence of $>10\%$,¹ is crucial with respect to large artery complications such as aortic aneurysm, aortic dissection, and/or large artery stenosis.^{2–5} The recently published European League Against Rheumatism (EULAR) recommendations for the use of imaging in LVV in clinical practice highlight the potential role of magnetic resonance imaging (MRI), especially in evaluating cranial arteries for GCA diagnosis as well as mural inflammation and/or luminal changes in patients with suspected TA including aortic involvement.⁶ In addition, MRI may be used for detection of giant cell aortitis, which is however recommended on the basis of expert opinion due to limited level of evidence.⁶ Given the frequently unspecific clinical appearance of patients with a potential differential diagnosis of aortitis, whole-body metabolic imaging with 2-[^{18}F]-fluoro-2-deoxy-D-glucose (^{18}F -FDG) positron-emission tomography (PET)/computed tomography (CT) is increasingly used to identify LVV along with other possible serious pathology such as infections or tumours. ^{18}F -FDG PET/CT is an emerging powerful imaging technique to non-invasively diagnose extracranial LVV, including aortitis, with a reported sensitivity and specificity of up to 90% and 98%, respectively.^{7–9} The relatively high radiation exposure from PET/CT warrants careful consideration in younger patients with TA where other diagnostic techniques may be preferable. Recently introduced fully integrated ^{18}F -FDG PET/MRI is associated with significantly less radiation exposure and allows the exact combination of ^{18}F -FDG PET and vascular MRI in a one-stop-shop multiparametric procedure for contemporaneous assessment of disease activity and extent together with possible late/chronic structural LVV complications, such as aneurysms and/or vessel narrowing/occlusion, as shown by preliminary studies.^{10–12} With respect to the high costs and the complexity of operating and interpreting PET/MRI studies, it remains questionable though, whether PET/MRI gains widespread availability and application in the clinical setting.¹³ Although several hurdles prevent PET/MRI from being more widely

adopted, it undoubtedly opens new research possibilities by evaluating radiation-free MRI techniques against molecular PET data. Recently, T1-weighted (T1W) fat-suppressed (fs) three-dimensional (3D) turbo spin-echo black-blood MRI was considered as a valid and reproducible imaging technique to non-invasively visualise established hallmarks of vessel wall inflammation in LVV, i.e., concentric wall thickening and contrast enhancement of the vessel wall^{14,15}; however, so far these MRI inflammation markers have not been compared conclusively to molecular imaging of the vessel wall by ^{18}F -FDG PET at the same time using a fully integrated PET/MRI system. Besides, the optimal MRI imaging protocol and MRI sequence for visualisation of aortic vessel wall inflammation has still to be defined and remains an issue of ongoing research. T1W fs volumetric interpolated breath-hold examination (VIBE) with Cartesian sampling is a well-established radiofrequency spoiled 3D gradient echo sequence frequently applied in whole-body PET/MRI protocols due to its very short acquisition time and the possibility to assess the soft tissue and vasculature simultaneously.¹⁶ Thus, T1W VIBE has the potential to aid in the diagnosis and surveillance of inflammatory conditions such as vasculitis of the aorta.

The aim of the present study was to evaluate the feasibility and diagnostic performance of T1W 3D Cartesian VIBE MRI compared to ^{18}F -FDG PET in the diagnosis of aortitis using an integrated ^{18}F -FDG PET/MRI system.

Material and methods

Patients

^{18}F -FDG PET/MRI examinations of 28 consecutive patients with suspected active LVV, who had been referred by a rheumatologist were analysed retrospectively. Patients underwent ^{18}F -FDG PET/MRI during primary diagnostic evaluation ($n=22$) or during follow-up in case of suspicious relapse ($n=6$) between April 2013 and October 2016. All patients underwent further clinical follow-up (median 15 months; range 5–65 months) with additional follow-up imaging studies including PET/MRI, PET/CT, CT, and magnetic resonance angiography (MRA) in 15 cases. Patient characteristics are shown in [Table 1](#).

Table 1
Study population characteristics.

	PET positive study for aortitis (aortitis group)	PET negative study for aortitis (control group)	p-Value
Patients (n)	14	14	n.s.
Age, years (\pm SD)	58.3 \pm 16.9	66.4 \pm 15.2	0.1752 ^a
Male sex (%)	3 (21.4)	3 (21.4)	n.s.
Body mass index (\pm SD)	25.2 \pm 4.7	26.5 \pm 6.5	0.8542 ^a
Height, m (\pm SD)	1.7 \pm 0.1	1.7 \pm 0.1	0.8902 ^a
Active smoker (%)	3 (21.4)	2 (14.3)	1.0000 ^b
Former smoker (%)	4 (28.6)	1 (7.1)	0.3259 ^b
Hypertension (%)	9 (64.3)	7 (50)	0.7036 ^b
Diabetes (%)	1 (7.1)	2 (14.3)	1.0000 ^b
Hypercholesterolaemia (%)	3 (21.4)	3 (21.4)	n.s.
Cardiovascular disease (%)	5 (35.7)	2 (14.3)	0.3845 ^b
Family history of CVD (%)	1 (7.1)	2 (14.3)	1.0000 ^b
C-reactive protein, mg/dl (\pm SD)	3.4 \pm 3.4	3 \pm 2.4	0.7652 ^a
Erythrocyte sedimentation rate, mm/h (\pm SD)	36.8 \pm 29.2	27.9 \pm 26.1	0.4622 ^a
Takayasu arteritis (%)	3 (21.4)	–	–
Giant cell arteritis (%)	11 (78.6) ^c	4 (28.6) ^c	0.0213 ^b
Excluded large vessel vasculitis (%)	–	10 (71.4)	–
¹⁸ F-FDG activity, MBq (\pm SD)	312.5 \pm 45.3	325.1 \pm 54.7	0.5503 ^a
PET AC Time p.i., min (\pm SD)	124.9 \pm 32.5	122.9 \pm 33.7	1.000 ^a

Data are presented as mean.

CVD, cardiovascular disease; CRP, C-reactive protein (normal <0.5 mg/dl); ESR, erythrocyte sedimentation rate (normal <20 mm/h); AC, acquisition; p.i., post injection; n.s., not significant; SD, standard deviation.

^a Mann–Whitney U test.

^b Fisher's exact test.

^c Four patients had positive temporal artery biopsy (one in the aortitis group and three in the control group).

Ethics

Institutional ethics review board approval was obtained for all patients (permit 416/17S), and written informed consent was obtained from all participants for the purpose of anonymised evaluation and publication of their data. All reported investigations were performed according to the principles of the Helsinki Declaration and to national regulations.

PET/MRI acquisition

Imaging was performed using a Biograph mMR (Siemens Medical Solutions, Erlangen, Germany), which allows whole-body simultaneous acquisition of PET and 3 T MRI data. A vascular-specific PET/MRI protocol was applied considering recently published recommendations for imaging in LVV.^{6,17} Patients fasted for at least 6 hours before ¹⁸F-FDG injection (319 \pm 50 MBq). Blood glucose levels were <150 mg/dl in all patients. On average, four bed positions (acquisition time of 2–4 minutes) were acquired for each patient during PET. Axial T1W fs Cartesian VIBE sequences before and after contrast media administration (mean 26 \pm 1 ml Magnograf) covering the aorta with a total scan time of approximately 1 minute were performed. Additionally, whole-body contrast-enhanced MRA was performed approximately 3 minutes before the post-contrast T1W VIBE sequences; however, the analysis of luminal changes by MRA is not the subject of the present study. Detailed imaging parameters of T1W VIBE are presented in Table 2.

Standard of reference

The final clinical diagnosis of LVV (i.e., GCA or TA) was established by considering the American College of Rheumatology criteria, PET imaging and/or long-term clinical follow-up in an interdisciplinary consensus decision by two board-certified rheumatologists and one nuclear medicine physician. A diagnosis of LVV was based on typical clinical symptoms of cranial LVV (e.g., bi-temporal headaches, visual impairment, jaw claudication) and extra-cranial LVV

Table 2
Magnetic resonance imaging parameters.

	T1W Cartesian VIBE
Sequence	3D-GRE
Fat suppression	Q-fat saturation
Repetition time (ms)	3.29
Echo time (ms)	1.16
Section thickness (mm)	5
Matrix	320 \times 240
Field of view (mm)	460
% phase field of view	75
Phase oversampling (%)	0
Sections per slab	44
Section oversampling (%)	45.5
Averages	1
PEC	A>P
Voxel size (mm ³)	1.8 \times 1.4 \times 5
Flip angle (°)	9
Acquisition time (min:sec)	0:13
No. of excitations	1

VIBE, volumetric interpolated breath hold examination; 3D, three-dimensional; GRE, gradient echo; PEC, phase-encoding direction; A>P anterior to posterior.

(e.g., constitutional symptoms, dry cough, upper extremity claudication, polymyalgia symptoms, abdominal or back pain) in conjunction with a humoral inflammatory response (raised levels of C-reactive protein and/or erythrocyte sedimentation rate) and typical findings in PET (high smooth linear or long segmental ^{18}F -FDG uptake of the aorta and/or its main branches). All patients received further work-up to carefully exclude infectious disease and other autoimmune or malignant disorders. To evaluate the presence and extent of vascular inflammation within the aorta, PET served as the standard of reference for the final diagnosis of aortitis.

Image analysis

PET images were evaluated qualitatively by two nuclear medicine physicians in consensus with >10 years of PET experience comparing ^{18}F -FDG uptake of the aortic wall to ^{18}F -FDG uptake of the liver using a four-point visual grading scale (3=higher than liver uptake, 2=uptake similar to liver uptake, 1=uptake present, but lower than liver uptake, 0=no uptake).^{6,17} The aorta was divided into four segments (ascending aorta, aortic arch, descending thoracic aorta, and abdominal aorta) and each segment with an ^{18}F -FDG uptake of ≥ 2 was considered as positive for active aortitis.

With respect to the T1W VIBE MRI analysis, the paired pre- and post-contrast images of the same vessel segments were assessed by two experienced radiologists independently with >8 years of experience in reading vascular MRI studies. The readers were blinded to the clinical diagnosis, the laboratory findings, and the results of PET. The degree of inflammatory activity (IA) in each aortic segment was assessed considering concentric wall thickening (CWT) together with contrast enhancement of the vessel wall (CEW) using a four-point Likert scale (3=substantial, 2=moderate, 1=minimal, 0=none; Fig 1). Grades 1–3 within at least one segment of the aorta were considered as diagnostic for active aortitis. If the readers disagreed, the series were reviewed for a consensus decision.

Each aortic segment was also evaluated for image quality (IQ; 5=excellent, sharp delineation of the aorta without blurring; 4=good, exact delineation of the aorta with barely perceptible blurring; 3=acceptable, fair delineation of the aorta with minimal blurring; 2=poor, delineation of the aorta still possible with moderate to severe blurring; 1=non-diagnostic, severe blurring) and diagnostic confidence (DC; 5=excellent, exact diagnosis possible; 4=good, definite diagnosis possible; 3=acceptable, evaluation of major findings possible; 2=poor, evaluation still possible but limited; 1=missing, i.e. non-diagnostic) with a five-point Likert scale.

Statistics

Exact binomial and generalised estimating equation (GEE) model tests were applied to assess the diagnostic performance of T1W VIBE (i.e., sensitivity, specificity, positive predictive value, negative predictive value, and accuracy) on a patient- and segment-based analysis, respectively. Mann–Whitney *U* and Fisher's exact test were performed for unpaired samples to evaluate for differences in the distribution of metric and categorical variables, respectively. Cohen's kappa (*k*) was applied to test for interobserver reproducibility with respect to IA. The Cohen's *k* values are interpreted as: poor (*k* < 0), slight (*k* = 0–0.20), fair (*k* = 0.21–0.40), moderate (*k* = 0.41–0.60), substantial (*k* = 0.61–0.80) and almost perfect (*k* = 0.81–1). Spearman's rank correlation coefficient (*r*) was calculated to examine correlations between IQ and DC as well as IA and qualitative analysis in PET, respectively. Kruskal–Wallis test and Dunn's multiple comparison test were performed to test for differences between aortic segments regarding IQ and DC. All statistics were performed using MedCalc (version 18.5), R (version 3.5.0) and Prism 8 (version 8.0.1). *p*-Values of 0.05 or less were considered to be statistically significant.

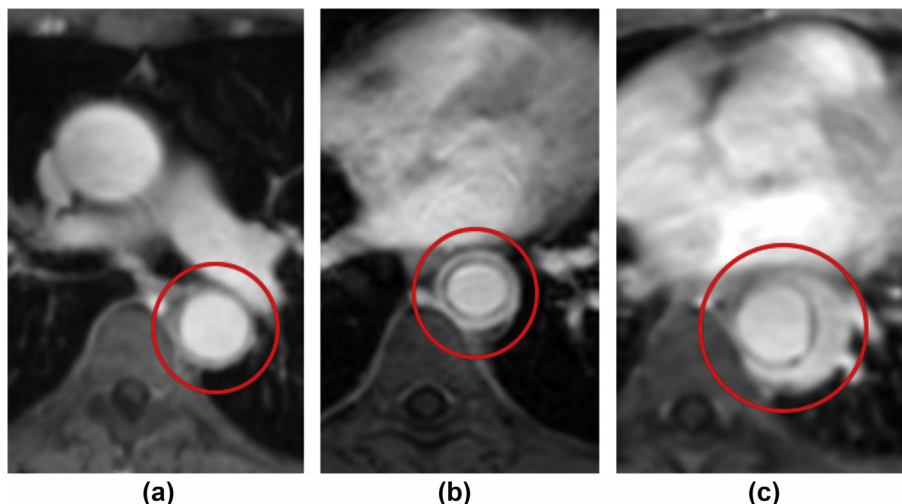


Figure 1 Degree of IA at the level of the descending thoracic aorta. (a) minimal IA, (b) moderate IA, and (c) substantial IA.

Results

Patient groups

According to the interdisciplinary consensus decision and particularly to the results of ^{18}F -FDG PET, 14 patients had positive PET indicating aortitis (11 active GCA, three active TA; Fig 2) and 14 patients had a negative study for aortitis (two active cranial GCA with temporal artery involvement, two inactive cranial GCA, and 10 without LVV). Thus, 14 patients were included into the aortitis group and 14 patients into the control group (without aortitis) for retrospective data analysis. ^{18}F -FDG PET/MRI was performed in the presence of corticosteroid treatment (range 5–15 mg/day within the week of the examination) in eight patients of the aortitis group (57.1%) and five patients of the control group (35.7%), respectively. The prevalence of cardiovascular risk factors was comparable for both groups. Study population characteristics are summarised in Table 1.

Diagnostic performance of T1W VIBE in comparison to ^{18}F -FDG PET

Comparing T1W 3D VIBE and the standard of reference ^{18}F -FDG PET on a patient-based analysis, MRI was true positive in 12 patients, false negative in two patients, true negative in 14 patients and false positive in none of the patients, resulting in a sensitivity, specificity, positive

predictive value, negative predictive value, and accuracy of 85.7%, 100%, 100%, 87.5% and 92.9%, respectively, based on exact binomial test. On a segment-based analysis, MRI was true positive in 29 aortic segments, false negative in 20 aortic segments, and true negative in 62 aortic segments without false-positive results (one segment, i.e. aortic arch, was excluded from overall analysis due to non-diagnostic image quality in MRI). Thus, based on GEE model test, sensitivity, specificity, positive predictive value, negative predictive value, and accuracy were 59.8%, 100%, 100%, 68% and 82.1%, respectively. The highest sensitivity was seen in the abdominal aorta (92.3%), whereas lower sensitivities were observed in the ascending aorta (25%), the aortic arch (50%), and the descending thoracic aorta (66.7%). In view of IA, CWT of the aorta as a hallmark of vasculitis was always seen together with significant CEW (Figs 3 and 4) in the aortitis group, whereas CWT and/or CEW were missing in the control group (Tables 3 and 4). Besides, a significant correlation of IA with the degree of ^{18}F -FDG aortic wall uptake in PET could be demonstrated (Spearman's $r=0.679$; $p<0.0001$).

Image quality, diagnostic confidence, and interobserver agreement

IQ and DC were acceptable to good in all examinations (mean 3.4 ± 0.8 and 3.7 ± 0.9 , respectively) without a significant difference between the aortitis group and the

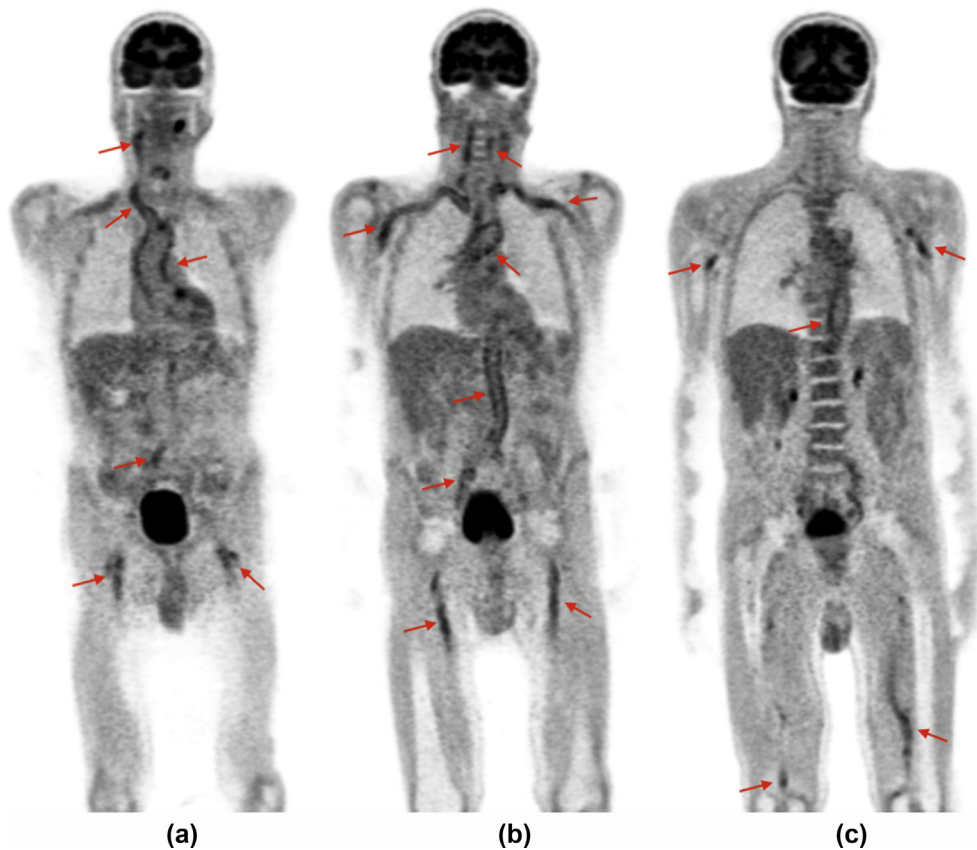


Figure 2 Coronal PET images in different planes (a–c) show extensive large vessel vasculitis with aortitis and inflammation of the aortic branches including peripheral arteries (grade 3 ^{18}F -FDG uptake; see red arrows) in a 75-year-old patient with giant cell arteritis.

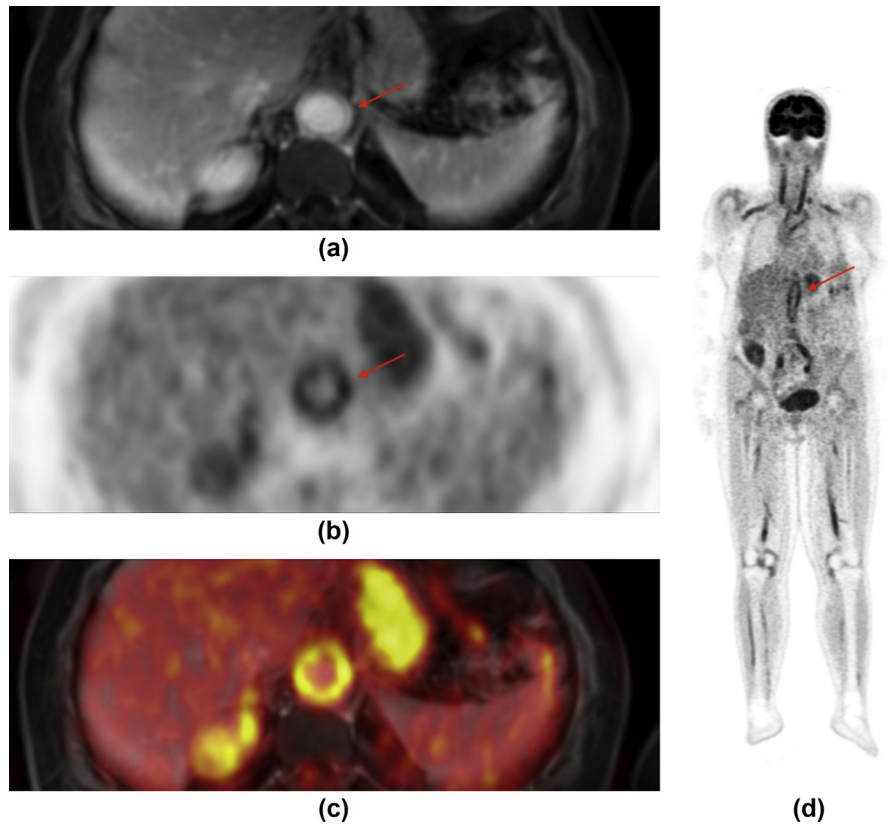


Figure 3 In a 65-year-old patient with giant cell arteritis (a) axial T1W VIBE at the level of the upper abdomen shows CWT with significant CEW of the abdominal aorta (red arrow) as well as pathological mural ^{18}F -FDG uptake (b; red arrow) in perfect correlation with MRI (c) suggesting active aortitis. (d) The corresponding coronal PET image shows extensive large vessel vasculitis in the aorta (red arrow at the level of image a–c), main branches and even in the femoral arteries.

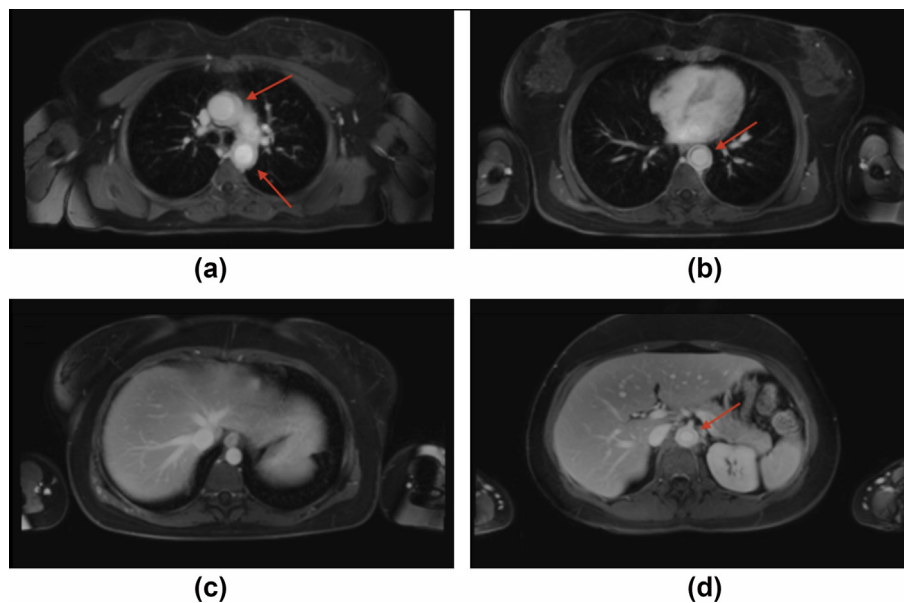


Figure 4 Axial contrast-enhanced T1W VIBE in a 33-year-old patient with Takayasu aortitis shows the segmental nature of vasculitis affecting (a) the aortic arch (red arrows), (b) the upper descending thoracic aorta (red arrow), and (d) the abdominal aorta (red arrow) without affecting (c) the distal part of the descending thoracic aorta (CWT with CEW is missing).

Table 3

Comparison of MRI inflammatory activity scores and qualitative PET scores in all vessel segments of the aortitis group.

No.	MRI inflammatory activity score				PET visual grading scale			
	AA	AAR	DA	ABA	AA	AAR	DA	ABA
1	3	1	3	3	3	2	3	3
2	0	0	0	3	3	3	3	3
3	0	0	0	0	2	2	2	1
4	0	1	2	1	3	3	3	3
5	3	2	1	2	3	3	3	3
6	0	1	1	1	3	3	3	3
7	0	^a	0	1	1	^a	1	3
8	0	0	0	1	2	3	3	3
9	1	1	1	1	3	3	3	3
10	0	0	0	0	2	2	2	2
11	0	0	1	1	1	1	2	2
12	0	0	0	3	3	2	1	3
13	0	1	1	3	3	3	3	3
14	0	0	1	1	3	3	3	3

^aNot included in statistical analysis due to non-diagnostic image quality in MRI.

AA, ascending aorta; AAR, aortic arch; DA, descending thoracic aorta; ABA, abdominal aorta.

control group according to Mann–Whitney *U* testing, respectively. The highest IQ and DC were observed in the abdominal aorta (mean 3.8±0.7 and 4.1±0.7, respectively) and the lowest in the ascending aorta (mean 3.1±0.7 and 3.3±0.8, respectively) with significant differences according to the Kruskal–Wallis test ($p=0.0080$ for IQ, $p=0.0011$ for DC), apparently having impact on sensitivity of T1W VIBE in the different aortic segments (Fig 5). Besides, both IQ and DC were correlated to each other (Spearman's $r=0.763$; $p<0.0001$). Finally, a substantial interobserver agreement was shown for the identification of aortic IA (Cohen's $k = 0.69$).

Discussion

This is the first study evaluating the diagnostic performance of gradient echo MRI by T1W fs 3D Cartesian VIBE for the diagnosis of aortitis using fully integrated ¹⁸F-FDG PET/MRI and ¹⁸F-FDG PET as the standard of reference for the assessment of inflammatory aortic involvement. The results of this retrospective feasibility study demonstrate that T1W VIBE MRI of the aorta detects vessel wall inflammation in a comparable number of patients with LVV in relation to ¹⁸F-FDG PET, highlighting its potential of aiding in the diagnostic work-up of patients with extracranial aortic involvement.

Table 4

Comparison of magnetic resonance imaging (MRI) inflammatory activity scores and qualitative positron-emission tomography (PET) scores between the aortitis group and the control group.

	Aortitis group	Control group	p
MRI inflammatory activity score (±SD)	0.8±1	0	0.0001 ^a
PET visual grading scale (±SD)	2.5±0.8	0.6±0.5	0.0001 ^a

Data are presented as mean.

Relationship between sensitivity, diagnostic confidence and image quality

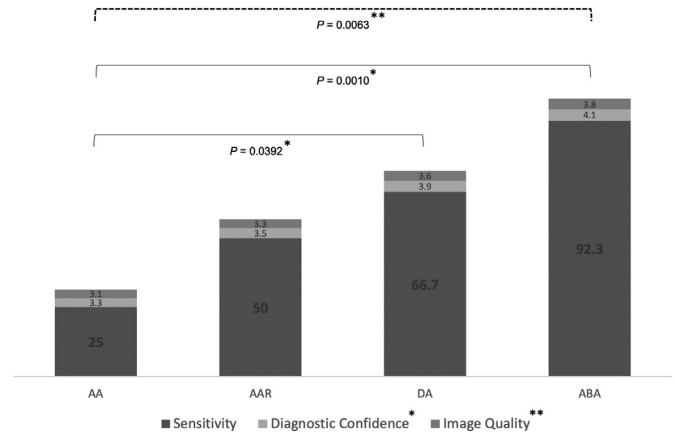


Figure 5 Sensitivity, diagnostic confidence, and image quality in the different aortic segments. Data regarding sensitivity are in percent, whereas scores of diagnostic confidence and image quality are presented as mean values. Kruskal–Wallis test showed significant results with respect to image quality and diagnostic confidence in the different aortic segments ($p=0.0080$ and 0.0011 , respectively). After performing Dunn's multiple comparison test, significant differences were shown between AA and ABA regarding image quality (dotted line) and between AA and ABA as well as AA and DA considering diagnostic confidence (solid line), respectively. AA=ascending aorta; AAR=aortic arch; DA=descending thoracic aorta; ABA=abdominal aorta.

Early imaging is recommended in patients with LVV, with ultrasound and MRI being the first choices particularly in patients with suspected cranial GCA and TA, respectively⁶; however, in patients with potential inflammatory large vessel involvement including the aorta, ultrasound is of limited value and lacks of standardised criteria. Therefore, it is not suggested for the evaluation of aortitis by the current EULAR recommendations.⁶ By contrast, cross-sectional and functional imaging techniques such as MRI, CT, and/or PET/CT offer the possibility to assess the whole aorta without superimpositions by bone, air or bowel gas, respectively. Due to radiation exposure, low soft-tissue contrast, and potential adverse effects of iodinated contrast media, CT is limited, whereas PET/CT is restricted by high costs, limited availability, and radiation burden. The advantages of MRI are the absence of radiation and the simultaneous detection of vessel wall thickening and contrast enhancement together with wall oedema, which are presumed to reflect active inflammation. Vessel wall MRI by T1W two-dimensional (2D) and 3D (turbo) spin-echo black-blood sequences has been evaluated in patients with LVV/aortitis in several reports, whereas validated data for gradient echo MRI are lacking, although their application for aortic wall imaging is recommended^{14,15,18–20}; however, MRI sequences in these studies suffer from reference standard limitations, i.e., missing of a comprehensive reference standard including ¹⁸F-FDG PET.

Molecular imaging by ^{18}F -FDG PET has shown its great potential in detecting inflammatory changes in the aorta and its branches in the early disease phase, potentially preceding structural vessel wall changes as shown by MRI.^{12,18,21–23} Besides, ^{18}F -FDG PET provides complementary and distinctive data compared to clinical assessment in LVV, potentially predicting future clinical relapse.⁸ Thus, ^{18}F -FDG PET was chosen as the standard of reference to evaluate T1W VIBE with CWT and CEW as typical hallmarks of vasculitis using a fully integrated PET/MRI system. To the authors' knowledge, vessel wall MRI has been compared to ^{18}F -FDG PET/CT in a few small-sized studies, but evaluation of comparative simultaneously acquired PET and MRI data were still missing.^{18,24,25}

According to the present results, T1W VIBE showed excellent concordance with ^{18}F -FDG PET on a patient-based analysis resulting in a sensitivity of 85.7%, specificity of 100%, and an overall diagnostic accuracy of 92.9%, respectively. ^{18}F -FDG uptake in the aortic wall of at least equal to the liver uptake was considered positive for active aortitis. This is a common and very sensitive approach, but potentially bears limitations with respect to specificity, given the well-known ability of atherosclerotic plaques in accumulating ^{18}F -FDG²⁶; however, ^{18}F -FDG uptake in atherosclerosis is more focal and less intense compared to the very smooth, linear, and intense uptake in patients suffering from aortitis, which is typical for active vasculitis. In addition, the prevalence of cardiovascular disease was relatively low with 25% in the present study population, making a significant impact of atherosclerosis on qualitative PET results unlikely.

Notably, increased CWT always appeared together with CEW, suggesting that both signs appear coincidentally in LVV patients with disease onset or disease flare. In the control group, T1W VIBE did not show CWT and/or CEW, underlining the specificity of these inflammation markers, which is in line with previous reports.^{14,15} Indeed, CWT together with CEW was significantly correlated to qualitative vessel wall scores in ^{18}F -FDG PET; however, the relationship was only moderate as a substantial portion of MRI positive patients with grade 3 vessel wall uptake in ^{18}F -FDG PET demonstrated only low IA values, indicating that the degree of CWT together with CEW may be limited in showing the correct level of vessel wall inflammation with potential underestimation of disease activity. This is confirmed by the finding that in nearly all patients with grade 2 ^{18}F -FDG vessel wall uptake, MRI was negative with respect to IA, suggesting a potential role of ^{18}F -FDG PET in showing low-grade inflammation. These findings are supported by results in the current literature, indicating that ^{18}F -FDG PET is potentially valuable in showing subclinical active vasculitis.^{8,9} Nevertheless, CWT and CEW are useful hallmarks of vessel wall inflammation to establish the diagnosis of LVV/aortitis; however, their value in monitoring of vasculitis is still debated and requires further attention, as MRI data on this topic are controversial compared to laboratory or clinical markers.²⁷ Hence, large prospective trials are needed to evaluate the role of MRI in monitoring the course of LVV/aortitis.

Conventional 3D T1W fs VIBE using Cartesian sampling plays a well-established role in MRI of the abdomen; however, the utility of this sequence depends on the ability of patients to hold their breath, as respiratory motion artefacts can cause significant blurring. In the present study, at least acceptable image quality was obtained in most of analysed vessel segments due to sufficient breath-holding, achieving the best IQ and DC in the abdominal aorta. This was expected, as aortic elasticity and pulsatility decrease in the lower parts of the aorta with consecutively less motion artefacts next to absence of heart and respiratory pulsation artefacts, respectively.²⁸ In contrast, the worst IQ and DC were obtained in the ascending aorta, which is substantially exposed to pulsation of the heart. Indeed, sensitivity of T1W VIBE appeared to be related to IQ and DC with poor results on a segment-based analysis in the upper parts of the aorta and excellent findings in the lower segments of the aorta. Navigated electrocardiogram- or pulse-triggered MRI sequences for the thoracic part of the aorta should be considered as a complementary approach to T1W VIBE in view of heart motion related artefacts and the consecutive potential risk of underestimating disease extent and activity in patients with aortitis. Nevertheless, T1W VIBE was able to demonstrate findings suggestive for thoracic aortitis in a noteworthy number of patients, especially in the descending thoracic aorta.

As this was a retrospective single-centre study with a small number of patients, data have to be interpreted carefully. Ideally, this study would have included an age, gender, and atherosclerotic risk factor-matched control group without any features of LVV; however, by recruiting control subjects from patients who initially were suspected of having LVV/aortitis but finally were diagnosed as not having aortitis, the present study setting comes closer to the daily routine that confronts clinicians. Additionally, histological evidence of LVV is missing in most cases, but the clinical value of temporal artery biopsy has been debated in the presence of imaging and biopsy of the aorta is only available in patients undergoing surgery.^{29,30} Moreover, in the present study, only the aorta was evaluated without the main branch arteries due to limited resolution of applied T1W VIBE for smaller vessels. Finally, a substantial portion of patients received low dose glucocorticoid treatment at the time of image acquisition, which may decrease ^{18}F -FDG vessel wall uptake and IA in MRI resulting in potential underestimation of disease activity and extent. Nevertheless, substantial degrees of vessel wall inflammation were shown in all patients with aortitis despite glucocorticoid therapy, making a significant impact on PET and MRI results unlikely.

In conclusion, vessel wall imaging by T1W fs 3D Cartesian VIBE MRI allows diagnosis of aortitis in a comparable number of patients in relation to ^{18}F -FDG PET as the standard of reference. Limitations in sensitivity were observed in the thoracic part of the aorta due to motion artefacts, necessitating navigated ECG- or pulse triggered MRI sequences for this region. T1W VIBE may aid in the management of patients with LVV and should be considered as a complementary approach in LVV specific MRI protocols at

least for evaluating the abdominal part of the aorta due to its high accuracy and quick performance.

Conflict of interest

The authors declare no conflict of interest.

References

- Slobodin G, Naschitz JE, Zuckerman E, et al. Aortic involvement in rheumatic diseases. *Clin Exp Rheumatol* 2006;**24**(2 Suppl. 41):S41–7.
- Gonzalez-Gay MA, Garcia-Porrúa C, Pineiro A, et al. Aortic aneurysm and dissection in patients with biopsy-proven giant cell arteritis from northwestern Spain: a population-based study. *Medicine (Baltimore)* 2004;**83**(6):335–41.
- Evans JM, O'Fallon WM, Hunder GG. Increased incidence of aortic aneurysm and dissection in giant cell (temporal) arteritis. A population-based study. *Ann Intern Med* 1995;**122**(7):502–7.
- Nuenninghoff DM, Hunder GG, Christianson TJ, et al. Incidence and predictors of large-artery complication (aortic aneurysm, aortic dissection, and/or large-artery stenosis) in patients with giant cell arteritis: a population-based study over 50 years. *Arthritis Rheum* 2003;**48**(12):3522–31.
- de Boysson H, Liozon E, Lambert M, et al. 18F-fluorodeoxyglucose positron emission tomography and the risk of subsequent aortic complications in giant-cell arteritis: a multicenter cohort of 130 patients. *Medicine (Baltimore)* 2016;**95**(26):e3851.
- Dejaco C, Ramiro S, Duftner C, et al. EULAR recommendations for the use of imaging in large vessel vasculitis in clinical practice. *Ann Rheum Dis* 2018;**77**(5):636–43.
- Soussan M, Nicolas P, Schramm C, et al. Management of large-vessel vasculitis with FDG-PET: a systematic literature review and meta-analysis. *Medicine (Baltimore)* 2015;**94**(14):e622.
- Grayson PC, Alehashemi S, Bagheri AA, et al. 18 F-Fluorodeoxyglucose-positron emission tomography as an imaging biomarker in a prospective, longitudinal cohort of patients with large vessel vasculitis. *Arthritis Rheumatol* 2018;**70**(3):439–49.
- Quinn KA, Ahlman MA, Malayeri AA, et al. Comparison of magnetic resonance angiography and (18)F-fluorodeoxyglucose positron emission tomography in large-vessel vasculitis. *Ann Rheum Dis* 2018 Aug;**77**(8):1165–71. <https://doi.org/10.1136/annrheumdis-2018-213102>. Epub 2018 Apr 17.
- Einspieler I, Thurmel K, Eiber M, et al. First experience of imaging large vessel vasculitis with fully integrated positron emission tomography/MRI. *Circ Cardiovasc Imaging* 2013;**6**(6):1117–9.
- Einspieler I, Thurmel K, Pyka T, et al. Imaging large vessel vasculitis with fully integrated PET/MRI: a pilot study. *Eur J Nucl Med Mol Imaging* 2015;**42**(7):1012–24.
- Einspieler I, Thurmel K, Eiber M. Fully integrated whole-body [18F]-fluorodeoxyglucose positron emission tomography/magnetic resonance imaging in therapy monitoring of giant cell arteritis. *Eur Heart J* 2016;**37**(6):576.
- Ehman EC, Johnson GB, Villanueva-Meyer JE, et al. PET/MRI: where might it replace PET/CT? *J Magn Reson Imaging* 2017;**46**(5):1247–62.
- Treitl KM, Maurus S, Sommer NN, et al. 3D-black-blood 3T-MRI for the diagnosis of thoracic large vessel vasculitis: a feasibility study. *Eur Radiol* 2017;**27**(5):2119–28.
- Wenter V, Sommer NN, Kooijman H, et al. Clinical value of [18F]FDG-PET/CT and 3D-black-blood 3T-MRI for the diagnosis of large vessel vasculitis and single-organ vasculitis of the aorta. *Q J Nucl Med Mol Imaging* 2018 Jan 2. <https://doi.org/10.23736/S1824-4785.18.03036-4> [Epub ahead of print].
- Ishii S, Hara T, Nanbu T, et al. Optimized workflow and imaging protocols for whole-body oncologic PET/MRI. *Jpn J Radiol* 2016;**34**(11):754–62.
- Slart R, Writing Group, Reviewer Group, et al. FDG-PET/CT(A) imaging in large vessel vasculitis and polymyalgia rheumatica: joint procedural recommendation of the EANM, SNMMI, and the PET Interest Group (PIG), and endorsed by the ASNC. *Eur J Nucl Med Mol Imaging* 2018;**45**(7):1250–69.
- Meller J, Strutz F, Siefker U, et al. Early diagnosis and follow-up of aortitis with [(18)F]FDG PET and MRI. *Eur J Nucl Med Mol Imaging* 2003;**30**(5):730–6.
- Choe YHHB, Koh EM, Do YS, et al. Takayasu's arteritis: assessment of disease activity with contrast enhanced MRA imaging. *AJR Am J Roentgenol* 2000;**175**:505–11.
- Baliyan V, Verdini D, Meyersohn NM. Noninvasive aortic imaging. *Cardiovasc Diagn Ther* 2018;**8**(Suppl. 1):S3–18.
- Hartlage GR, Palios J, Barron BJ, et al. Multimodality imaging of aortitis. *JACC Cardiovasc Imaging* 2014;**7**(6):605–19.
- Meller J, Grabbe E, Becker W, et al. Value of F-18 FDG hybrid camera PET and MRI in early Takayasu aortitis. *Eur Radiol* 2003;**13**(2):400–5.
- Versari A, Pipitone N, Casali M, et al. Use of imaging techniques in large vessel vasculitis and related conditions. *Q J Nucl Med Mol Imaging* 2018;**62**(1):34–9.
- Scheel AK, Meller J, Vosschenrich R, et al. Diagnosis and follow up of aortitis in the elderly. *Ann Rheum Dis* 2004;**63**(11):1507–10.
- Both M, Ahmadi-Simab K, Reuter M, et al. MRI and FDG-PET in the assessment of inflammatory aortic arch syndrome in complicated courses of giant cell arteritis. *Ann Rheum Dis* 2008;**67**(7):1030–3.
- Rudd JH, Warburton EA, Fryer TD, et al. Imaging atherosclerotic plaque inflammation with [18F]-fluorodeoxyglucose positron emission tomography. *Circulation* 2002;**105**(23):2708–11.
- Spira D, Xenitidis T, Henes J, et al. MRI parametric monitoring of biological therapies in primary large vessel vasculitides: a pilot study. *Br J Radiol* 2016;**89**(1058):20150892.
- Whitlock MC, Hundley WG. Noninvasive imaging of flow and vascular function in disease of the aorta. *JACC Cardiovasc Imaging* 2015;**8**(9):1094–106.
- Salvarani C, Silingardi M, Ghirarduzzi A, et al. Is duplex ultrasonography useful for the diagnosis of giant-cell arteritis? *Ann Intern Med* 2002;**137**(4):232–8.
- Karassa FB, Matsagas MI, Schmidt WA, et al. Meta-analysis: test performance of ultrasonography for giant-cell arteritis. *Ann Intern Med* 2005;**142**(5):359–69.